

# A Monte-Carlo METHOD FOR MAKING SDSS *U*-BAND MAGNITUDE MORE ACCURATE

JIAYIN GU<sup>1</sup>, CUIHUA DU<sup>2</sup>, WENBO ZUO<sup>2</sup>, YINGJIE JING<sup>2</sup>, ZHENYU WU<sup>3</sup>, JUN MA<sup>3</sup> AND XU ZHOU<sup>3</sup>

<sup>1</sup>Department of Physics, Wuhan University of Technology, Wuhan 430000, P. R. China; gujiayin12@mails.ucas.ac.cn

<sup>2</sup>School of Physical Sciences, University of Chinese Academy of Sciences, Beijing 100049, P. R. China; ducuihua@ucas.ac.cn

<sup>3</sup>Key Laboratory of Optical Astronomy, National Astronomical Observatories, Chinese Academy of Sciences, Beijing 100012, P. R. China

*Draft version July 8, 2016*

## ABSTRACT

We develop a new Monte-Carlo-based method to convert the SDSS (Sloan Digital Sky Survey) *u*-band magnitude to the SCUSS (South Galactic Cap of *u*-band Sky Survey) *u*-band magnitude. Due to more accuracy of SCUSS *u*-band measurements, the converted *u*-band magnitude becomes more accurate comparing with the original SDSS *u*-band magnitude, in particular at the faint end. The average *u* (both SDSS and SCUSS) magnitude error of numerous main-sequence stars with  $0.2 < g - r < 0.8$  increase as *g*-band magnitude becomes fainter. When  $g = 19.5$ , the average magnitude error of SDSS *u* is 0.11. When  $g = 20.5$ , the average SDSS *u* error is up to 0.22. However, at this magnitude, the average magnitude error of SCUSS *u* is just half as much as that of SDSS *u*. The SDSS *u*-band magnitudes of main-sequence stars with  $0.2 < g - r < 0.8$  and  $18.5 < g < 20.5$  are converted, therefore the maximum average error of converted *u*-band magnitudes is 0.11. The potential application of this conversion is to derive more accurate photometric metallicity calibration from SDSS observation, especially for those distant stars. Thus, we can explore stellar metallicity distributions either in the Galactic halo or some stream stars.

*Subject headings:* stars:fundamental parameters-methods:data analysis-star:statistics

## 1. INTRODUCTION

It is an increasing perception that the Galactic halo system comprises at least two spatially overlapping components with different kinematics, metallicity and spatial distribution (Carollo et al. 2007, 2010; An et al. 2013, 2015). Chemical abundance is the direct observational ingredient in investigating the dual nature of the Galactic halo. Since the chemical abundance of stars have strong effect on the emergent flux, especially at blue end, the natural endeavor is to recover the metal information from large photometric surveys such as SDSS (Sloan Digital Sky Survey; York et al. 2000). The advantage of photometric metallicity estimate is that the metallicity information of large numbers of stars can be obtained.

Based on the SDSS *ugriz* photometry, Ivezić et al. (2008) used polynomial-fitting method from spectroscopic calibration of de-reddened  $u - g$  and  $g - r$  colors to derive the photometric metallicity (see also Peng et al. 2012). However, due to the relatively large error of SDSS *u*-band magnitude, only the metallicities [Fe/H], of stars brighter than  $g = 19.5$  are obtained. Combining the more accurate SCUSS (Zhou et al. 2016) *u*-band photometry, SDSS *g* and *r* photometry, Gu et al. (2015) developed a three-order polynomial photometric metallicity estimator, in which *u*-band magnitude can be used to faint magnitude of  $g = 21$ . However, both estimator developed by Ivezić et al. (2008) and Gu et al. (2015) based on polynomial-fitting have their intrinsic drawback that they can not be extended to metal-poor end. In order to solve this problem, Gu et al. (2016) (hereafter denoted as Paper I) devised a Monte-Carlo method to estimate stellar metallicity distribution function (MDF) which appears particularly good at both metal-rich and metal-poor ends. The natural forward step is to combine the SCUSS *u*, SDSS *g*, *r* photometry with the method introduced in Paper I to investigate the MDF of the Galactic halo stars. But only those stars in South Galactic cap are surveyed by SCUSS. How can we estimate the photometric metallicity distribution of faint stars (deep in Galactic halo) in both South and North hemisphere? This paper pro-

vides a new method to achieve this goal. Due to the fact that SCUSS *u* is more accurate than SDSS *u*, we convert SDSS *u* to SCUSS *u* using a Monte-Carlo method, through which we make the converted *u* magnitude becomes as accurate as SCUSS *u* magnitude.

We organize this paper as follows. In Section 2, we take a brief overview of the SDSS and SCUSS. The technical details for converting SDSS *u* to SCUSS *u* are presented in section 3. Section 4 evaluate the effectiveness of this conversion. The discussion of the potential application of the conversion is given in Section 5.

## 2. SDSS AND SCUSS

The SDSS is a digital multi-filter imaging and spectroscopic redshift survey using a dedicated 2.5 m wide-angle optical telescope at Apache Point Observatory in New Mexico, United States (Gunn et al. 2006). It began operation in 2000, and finally over 35% of the sky is covered, with about 500 million photometrically surveyed objects and more than 3 million spectroscopically surveyed objects. Five bands (*u*, *g*, *r*, *i*, and *z*) are used to simultaneously measure the objects magnitude, respectively with the effective wavelength of 3551, 4686, 6165, 7481, and 8931 Å. The limit magnitudes of *u*, *g*, *r*, *i*, and *z* are 22.0, 22.2, 22.2, 21.3, and 20.5, respectively (Abazajian et al. 2004). The relative photometric calibration accuracy for *u*, *g*, *r*, *i*, and *z* are 2%, 1%, 1%, 1% and 1%, respectively (Padmanabhan et al. 2008). Other technical details about SDSS can be found on the SDSS website <http://www.sdss3.org/>, which also provide interface for the public data access.

The South Galactic Cap *u*-band Sky Survey (SCUSS) is an international cooperative project that is jointly undertaken by National Astronomical Observatories of China and Steward Observatory of University of Arizona. It utilizes the 2.3 m Bok telescope located on Kitt Peak to photometrically survey the stars in the South Galactic Cap in *u* band with effective wavelength of 3538 Å. This project started in the

TABLE 1  
BRIEF SUMMARY OF SCUSS

Telescope	2.3 m Bok telescope
Site	Kitt Peak in Arizona
CCD	2×2 4k×4k CCD array
Exposure time	300 s
Filter Wavelength	3538 Å
Filter FWHM	520 Å
Magnitude Limit	23.2 mag
Survey Area	~ 5000 deg <sup>2</sup>
Observation Period	2010~2013

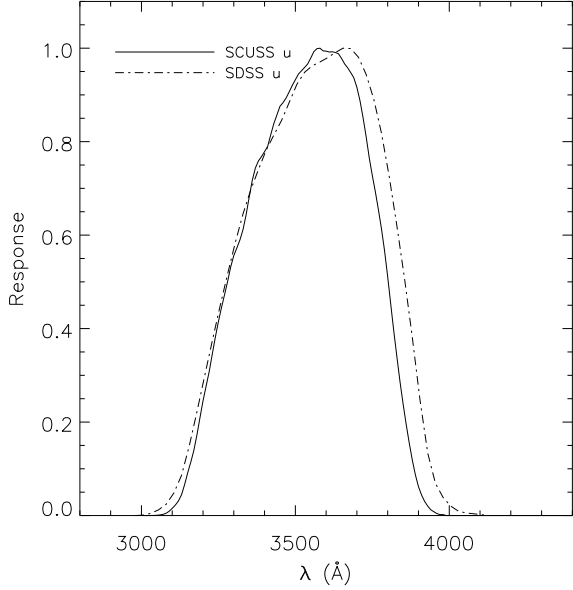


FIG. 1.— Response curves of both the SCUSS  $u$  and the SDSS  $u$  filters. Atmospheric extinction at the airmass of 1.3 is taken into account, and both curves are normalized to their maxima.

summer of 2009, began its observation in the fall of 2010, completed in the fall of 2013, and finally about 5000 deg<sup>2</sup> area ( $30^\circ < l < 210^\circ$ ,  $-80^\circ < b < -20^\circ$ ) were surveyed. Its main goal is to provide the essential input data to the Large Sky Area Multi-Object Fiber Spectroscopic Telescope (LAMOST) project (Zhao et al. 2006). Figure 1 shows the similarity in response curve between the  $u$  band filter of SCUSS and that of SDSS. The limit magnitude for point sources is about 23.2 mag with a 5-minute exposure time, and is about 1.5 mag deeper than that of SDSS  $u$  band magnitude (Jia et al. 2014; Peng et al. 2015). In Table 1, we provide a brief summary of SCUSS. The more detailed information and data reduction about SCUSS can be found in Zhou et al. (2016); Zou et al. (2015, 2016), and the SCUSS website <http://batc.bao.ac.cn/Uband/>, which also provides information for public data access.

As shown in Figure 2, the average error of SCUSS  $u$  and SDSS  $u$  of numerous main-sequence stars with  $0.2 < g - r < 0.8$  are plotted as functions of  $g$ -band magnitude. It clearly shows that the error of SDSS  $u$  is much larger than that of SCUSS  $u$  on the whole, especially at the faint end. The spectroscopically surveyed stars has limiting magnitude of  $g = 19.5$ . Coincidentally, the error of SDSS  $u$  limits the ap-

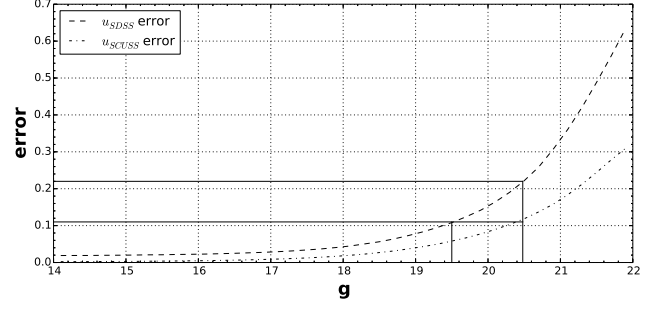


FIG. 2.— Average  $u$  (SDSS and SCUSS) error as a function of  $g$ -band magnitude. Main-sequence stars with  $0.2 < g - r < 0.8$  are selected. It is obvious that the error of SDSS  $u$  is much larger than that of SCUSS  $u$ , especially at the faint end.

plication of photometric metallicity estimates in the range of  $g < 19.5$ . From Figure 2, we find that the error of SDSS  $u$  is about 0.11 when  $g = 19.5$ . So we set 0.11 as the maximum error. Beneath the error of 0.11, the SCUSS  $u$  corresponds to the range of  $g < 20.5$ . However, the SDSS  $u$  error is up to 0.22 when  $g = 20.5$ . In the following, we will convert SDSS  $u$  to SCUSS  $u$  for stars brighter than  $g = 20.5$  so that the error of converted  $u$  don't exceed 0.11. Here, we only convert the SDSS  $u$  with  $18.5 < g < 20.5$  for main-sequence stars. Since  $g$ -,  $r$ -band magnitudes are much more accurate than  $u$ , we assume that they are absolutely precise, at least in the considered  $g$ -band magnitude range. So the error of  $u - g$  is the direct consequence of the error of  $u$ .

### 3. METHOD

For each object surveyed by SCUSS, we can identify the same object from SDSS catalog by matching their positions. So in the merged catalog, each star has the following information: position ( $ra$  &  $dec$ ), SCUSS  $u$ -band magnitude and its error, SDSS  $u$ ,  $g$ ,  $r$ ,  $i$ ,  $z$ -band magnitudes and their error and extinction. Here, the extinction for SDSS  $u$ -band magnitude is also used by SCUSS  $u$ -band magnitude. Throughout this paper, magnitudes and colors are understood that they have been corrected for extinction and reddening following Schlegel et al. (1998). We select the stars from SCUSS catalog by the following criteria:

1.  $18.5 < g < 20.5$ ;
2.  $0.2 < g - r < 0.8$ ;
3.  $0.6 < (u - g)_{SDSS} < 2.2$ ;
4.  $0.6 < (u - g)_{SCUSS} < 2.2$ ;
5. main-sequence stars are selected by only including those objects at distances smaller than 0.15 mag from the stellar locus described by the following equation (Jurić et al. 2008):

$$(g - r) = 1.39\{1 - \exp[-4.9(r - i)^3 - 2.45(r - i)^2 - 1.68(r - i) - 0.05]\}$$

6. we further refine the selection of main-sequence stars by only including those objects at distances smaller than 0.3 mag from the stellar locus described by the following equation (Jia et al. 2014):

$$(u - g)_{SDSS} = \exp[-(g - r)^2 + 2.8(g - r) - 1]$$

We divide the color range of  $0.2 < g - r < 0.8$  into 6 equal bins, and also divide the magnitude range of  $18.5 < g < 20.5$  into 20 bins. Thus, we totally get  $120 \times 0.1 \times 0.1$  mag<sup>2</sup> bins,

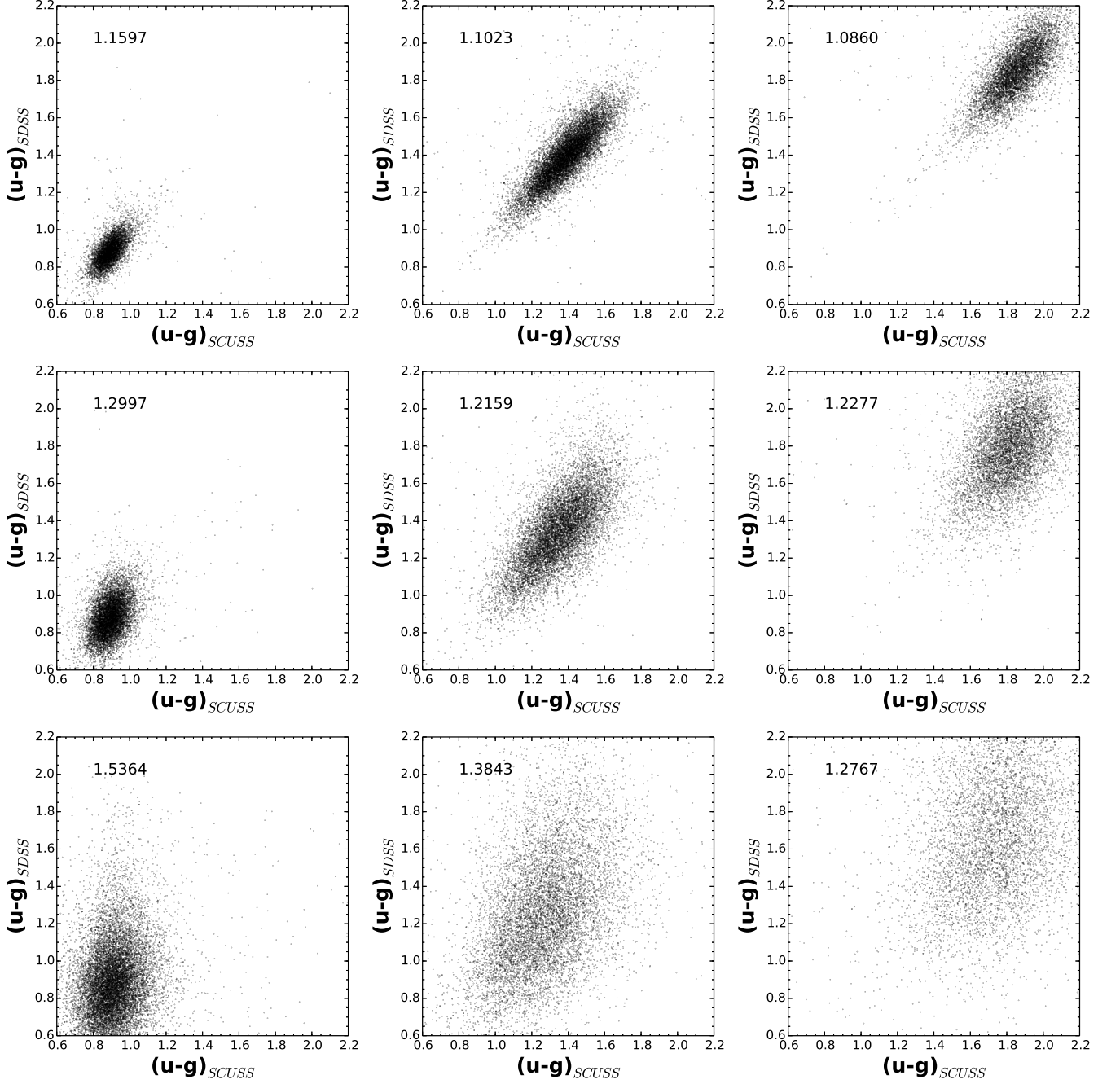


FIG. 3.— Two-color diagrams for  $(u-g)_{SCUSS}$  versus  $(u-g)_{SDSS}$ . Main-sequence stars in different magnitude and color range are selected. Stars for panels from top row to bottom row are with  $18.5 < g < 18.6$ ,  $19.4 < g < 19.5$  and  $20.4 < g < 20.5$  respectively. Stars for panels from left column to right column are with  $0.2 < g-r < 0.3$ ,  $0.5 < g-r < 0.6$  and  $0.7 < g-r < 0.8$  respectively. The numbers shown in each panel are the ratios of standard deviation between  $(u-g)_{SDSS}$  and  $(u-g)_{SCUSS}$ . These numbers are greater than one, which imply that SCUSS  $u$  is more accurate than SDSS  $u$ . Additionally, these numbers become larger as  $g$ -band magnitude becomes fainter, and the largest one corresponds to bottom left panel (blue and faint).

and designate each square bin by an *index* computed in the following manner:

$$index = \text{int}((u - g - 0.2)/0.1) * 20 + \text{int}((g - 18.5)/0.1)$$

where the symbol *int* stands for the integer portion. In this way the *index* takes value from 0 to 119. Main-sequence stars whose colors and magnitudes match a position specified by *index* will be used to construct a “converter”. Thus, we will totally obtain 120 converters, and each converter is denoted as *converter*[*index*]. In the following, each converter has the

form of  $16 \times 16$  array in which each element is further denoted as *converter*[*index*][*i*][*j*], where *i*, *j* range from 0 to 15. Each main-sequence star that is associated with one converter is further classified with two labels of integer number, *i* and *j*, which can be computed in the following manner:

$$i = \text{int}(((u - g)_{SDSS} - 0.6)/0.1)$$

$$j = \text{int}(((u - g)_{SCUSS} - 0.6)/0.1),$$

where the symbol *int* also stands for the integer portion. Each element in each converter array records the number of stars

whose  $(u-g)_{SDSS}$  and  $(u-g)_{SCUSS}$  colors match its position. We use `converter[index][i][:]` to denote the set of 16 numbers of `converter[index][i][j]` for  $j$  taking integer values from 0 to 15. The maximum value of the `converter[index][i][:]` is further denoted as  $max[index][i]$ .

Figure 3 shows the two-color diagrams for  $(u-g)_{SCUSS}$  versus  $(u-g)_{SDSS}$ . Main-sequence stars in different magnitude and color range are selected. Stars for panels from top row to bottom row are with  $18.5 < g < 18.6$ ,  $19.4 < g < 19.5$  and  $20.4 < g < 20.5$ , respectively. Stars for panels from left column to right column are with  $0.2 < g-r < 0.3$ ,  $0.5 < g-r < 0.6$  and  $0.7 < g-r < 0.8$ , respectively. Each one corresponds to one converter array. The more scattered the points in each panel, the larger error  $u$ -band magnitude it implies. As shown in Figure 3, the error of  $(u-g)_{SDSS}$  is larger than that of  $(u-g)_{SCUSS}$ , especially for those faint stars. The comparison of error for each panel is quantized by the ratio of standard deviation between  $(u-g)_{SDSS}$  and  $(u-g)_{SCUSS}$  that is shown. For the bottom left panel of the diagram, the ratio has the maximum value of 1.536 when comparing with others. This panel corresponds to the fainter and bluer stars that are reasonably belong to the Galactic halo.

The central idea for converting SDSS  $u$  to SCUSS  $u$  is that we obtain the color distribution of converted  $u-g$  according to the inputting distribution of  $(u-g)_{SDSS}$  and the scatter diagram in each panel of Figure 3. The scatter diagram of  $(u-g)_{SCUSS}$  versus  $(u-g)_{SDSS}$  is now explained as the consequence of probability. More points in a small region imply that a star have higher probability to locate in it. We reproduce a given distribution by the Monte-Carlo method. The converted  $u-g$  should be considered as same as  $(u-g)_{SCUSS}$ . Here, in order to distinguish the converted  $u-g$  from original  $(u-g)_{SDSS}$  and  $(u-g)_{SCUSS}$ , we denoted converted  $u-g$  with a subscript, namely  $(u-g)_{CONV}$ .

For  $n$  stars corresponding to  $index = a$ ,  $i = b$ , we generate  $n$  random numbers according to the distribution exhibited by the 15 numbers from `converter[a][b][0]` to `converter[a][b][15]`. The obtained  $n$  random numbers are all real numbers from 0 to 15. Then, the  $n$  random numbers are converted to  $(u-g)_{CONV}$  values by  $(u-g)_{CONV} = 0.1 * r + 0.6$ , where  $r$  is one random number. How to generate a sequence of random numbers that just comply with a given distribution? It is explained as follows. Suppose that there are two stochastic variables,  $X$  and  $Y$ , which can be assigned a random number generating function  $X = rand_X()$  and  $Y = rand_Y()$ , respectively. In each trial, we obtain a random number pair  $(X, Y)$ , where  $X$  is modulated to take the uniform-probability distributed random real number from 0 to 15. For any star, whose  $index$  and  $i$  has determined,  $Y$  is modulated to take the uniform-probability distributed random real number from 0 to  $max[index][i]$ . When  $Y \leq converter[index][i][int(X)]$  ( $int(X)$ , the integer portion of  $X$ ), we record  $X$  as a useful value, and otherwise discard it. By numerous trials, we obtain a sequence of random numbers  $\{X_1, X_2, X_3, \dots\}$  that follow the same probability distribution as those recorded in `converter[index][i][:]`. Here, because `converter[index][i][j]` can be equal to zero for some  $j$  values, we can discard them and record the non-zero elements and their positions in a new array. Through this method, the sampling efficiency can be improved greatly.

#### 4. TESTING

From the top three two-color diagrams of Figure 3, we find that  $(u-g)_{SDSS}$  may be expressed as a linear function of  $(u-g)_{SCUSS}$ . For the selected stars with  $18.5 < g < 18.6$ , the error

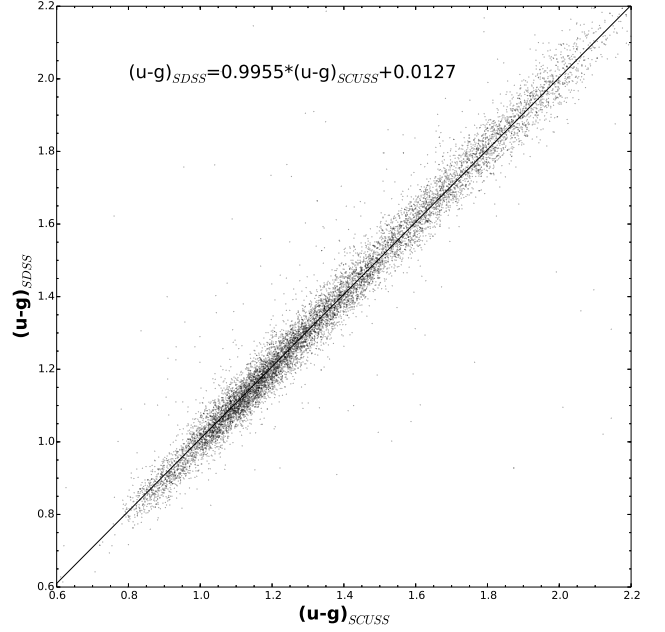


FIG. 4.— Two-color diagrams for  $(u-g)_{SCUSS}$  versus  $(u-g)_{SDSS}$ . Main-sequence stars with  $0.2 < g-r < 0.8$  and  $16.99 < g < 17.01$  are selected. The data are fitted with a linear line, with the expression shown in the figure. The slope almost equal to 1.

of  $u$  plays the minor role for the distribution of points in these diagrams. If the  $u$ -band (both SDSS and SCUSS) magnitudes were absolutely precise, the resulting transformation relation is supposed as follows:

$$(u-g)_{SDSS} = k * (u-g)_{SCUSS} + h,$$

where  $k$  is the slope and  $h$  represents a constant.

In evaluating which color (either  $(u-g)_{SDSS}$  or  $(u-g)_{SCUSS}$ ) has greater error, the reliability of the standard deviation ratio shown in Figure 3 depends on the assumption of  $k \approx 1$ . In Figure 4, we plot a two-color diagram of  $(u-g)_{SCUSS}$  versus  $(u-g)_{SDSS}$  for main-sequence stars with  $0.2 < g-r < 0.8$  and  $16.99 < g < 17.01$ . We also notice that the error of  $u$ -band magnitude at the bright magnitude  $g = 17$  is small, and therefore its effect on the color distribution in Figure 4 can be neglected. The trend of  $(u-g)_{SDSS}$  versus  $(u-g)_{SCUSS}$  is fitted by a line, with the expression shown in the figure. The slope  $k = 0.9955$  is almost equal to 1. The assumption of  $k \approx 1$  holds on. We can evaluate which  $u$  has greater error by dispersion degree of points in Figure 3. In addition, for convenience we may also approximately assume that SDSS  $u$  and SCUSS  $u$  are from the same photometric system, since they are almost similar if neglecting the error, as shown in Figure 4.

In order to evaluate the effect of this conversion, we plot the histograms of distribution of  $(u-g)_{SDSS}$ ,  $(u-g)_{SCUSS}$  and  $(u-g)_{CONV}$  for main-sequence stars with different magnitude and color ranges in Figure 5. The top three panels show color distribution of stars with  $18.5 < g < 19$ , the middle three with  $19.3 < g < 19.7$ , and the bottom three with  $20 < g < 20.5$ . Corresponding with the color range, stars for panels from left column to right column are with  $0.2 < g-r < 0.3$ ,  $0.5 < g-r < 0.6$  and  $0.7 < g-r < 0.8$ , respectively. The histograms in each panel are normalized to the maximum, with the actual peak values labeled. It is clear that the profiles



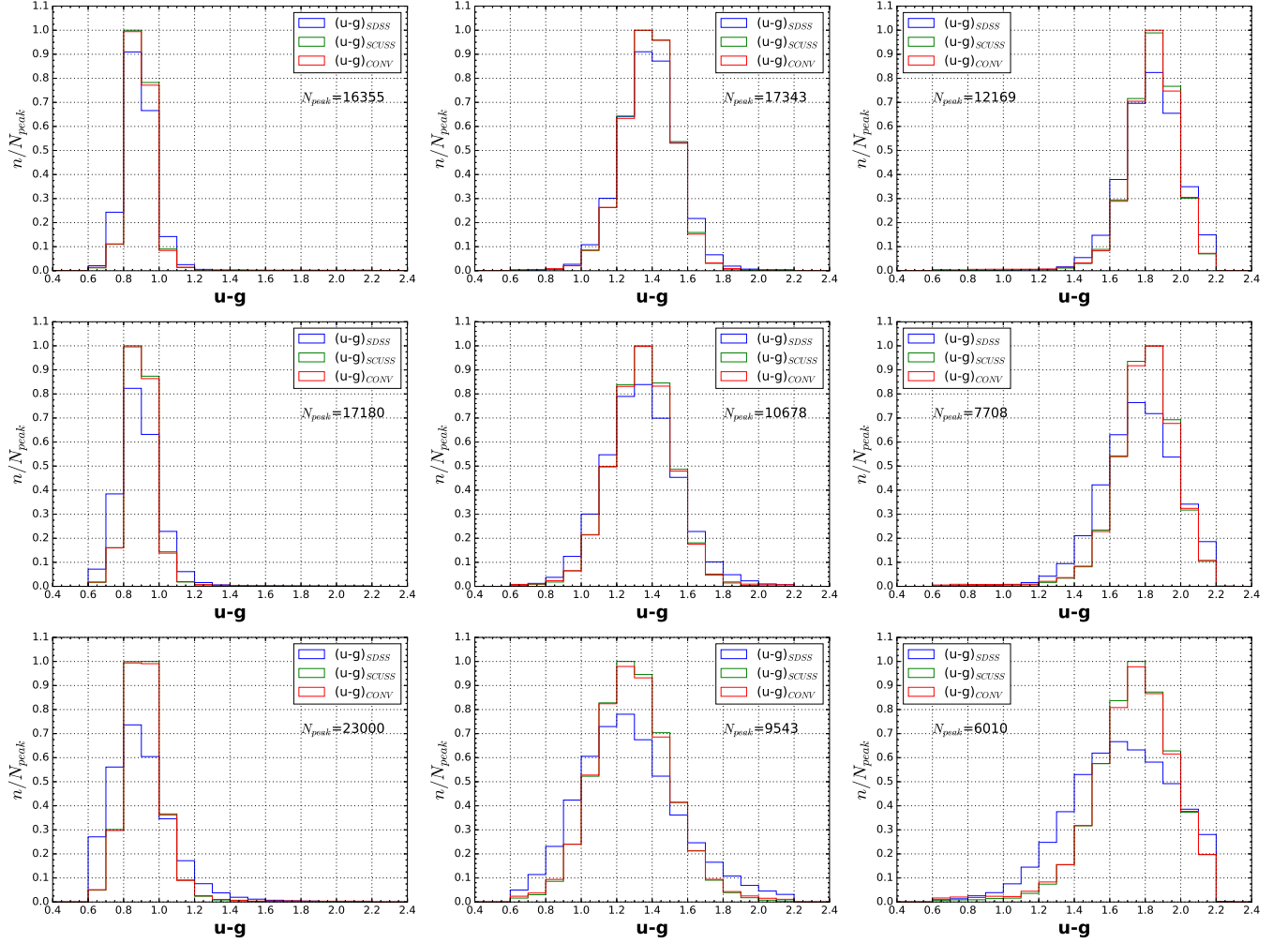


FIG. 5.— Histograms of distribution of  $(u-g)_{SDSS}$  (blue),  $(u-g)_{SCUSS}$  (green) and  $(u-g)_{CONV}$  (red) with different magnitude and color range. Stars for panels from top row to bottom row are with  $18.5 < g < 19$ ,  $19.3 < g < 19.7$  and  $20 < g < 20.5$ . Stars for panels from left column to right column are with  $0.2 < g-r < 0.3$ ,  $0.5 < g-r < 0.6$  and  $0.7 < g-r < 0.8$ , respectively. The histograms in each panel are normalized to the maximum, with actual peak values labeled. The histograms of  $(u-g)_{CONV}$  and histograms of  $(u-g)_{SCUSS}$  nearly coincide, directly reflecting the effectiveness of the conversion from SDSS  $u$  to SCUSS  $u$ .

of the histograms of  $(u-g)_{CONV}$  in each panel are almost same as those of  $(u-g)_{SCUSS}$ . This effect indicates that the conversion has the ability to make the error of  $u_{SDSS}$  smaller, as small as that of  $u_{SCUSS}$ . Actually, the distribution of  $(u-g)_{CONV}$  will completely coincide with that of  $(u-g)_{SCUSS}$  as long as the number of stars selected is large enough for the histogram. After all the convertor arrays are constructed by the data of SCUSS  $u$ . Thus, for larger sky area in which there have no SCUSS  $u$ , the convertor array could be used to make the error of SDSS  $u$  smaller. As a result, the error of the converted  $u$  magnitude when  $g = 20.5$  is equal to the original error of SDSS  $u$  when  $g = 19.5$ . However, we are still cautious that to what extent this conversion method can diminish the  $u$  magnitude error cannot be fully tested until a deeper survey is available.

## 5. DISCUSSION

As we all know,  $u$ -band measurements is very important to derive the photometric metallicity and therefore to construct a precise MDF. Because of the relatively shallow survey limit ( $u \sim 22$ ) and the relatively large error in the SDSS  $u$ -band near the faint end, the application of the photometric metallicity estimates is greatly restricted in the range of  $g < 19.5$ ,

an insufficient depth to explore the distant halo and substructures. However, the SCUSS  $u$  is 1.5 mag deeper than SDSS  $u$ , and its error is smaller than SDSS  $u$  error on the whole. The potential application of the conversion from SDSS  $u$  to SCUSS  $u$  is very important to derive relative accurate photometric metallicities of distant stars. In Paper I, we developed a new method to estimate the photometric metallicity distribution of large number of stars. Compared with other photometric calibration methods, this method in Paper I effectively reduces the error induced by the method itself, and therefore enables a more reliable determination of the photometric MDF. However, another error source still matters: the error of SDSS  $u$ -band magnitude. This error behavior limits the application of the method in the range of  $g < 19.5$  in Paper I. This range is same as that of Ivezić et al.'s (2008) photometric metallicity estimator. The more accurate SCUSS  $u$ -band measurements guarantee the accuracy of the stellar distribution in  $u-g$  versus  $g-r$  panel, and it extends the application of method in Paper I to even fainter stars. Thus, the photometric MDF of distant stars such as halo stars or some stream stars can be estimated.

However, only the stars in South Galactic Cap are surveyed by SCUSS which have relatively more accurate  $u$  band mag-

nitude, how to derive the photometric metallicity of stars in the North Galactic hemisphere? The conversion from SDSS  $u$  to SCUSS  $u$  statistically diminish the error of  $u$ -band magnitude, which make it possible to estimate the photometric MDF of stars in the whole sky. In this study, we have done the conversion for stars in  $18.5 < g < 20.5$ . The conversion combined with the method introduced in Paper I enable us to estimate the photometric metallicity distribution function for stars at least in the range of  $g < 20.5$ , which is 1 mag deeper than that of spectroscopically-surveyed stars. So we can study the chemical structure of the Galactic halo more detailed. Besides the application described above, the more accurate  $u$  band magnitude from the conversion, can be applied to address other scientific issues.

#### ACKNOWLEDGMENTS

This work was supported by joint fund of Astronomy of the National Natural Science Foundation of China and the Chinese Academy of Science, under Grants U1231113. This work was also by supported by the Special funds of cooperation between the Institute and the University of the Chinese Academy of Sciences. In addition, this work was supported by the National Natural Foundation of China (NSFC, No.11373033, No.11373035), and by the National Basic Research Program of China (973 Program) (No. 2014CB845702, No.2014CB845704, No.2013CB834902).

We would like to thank all those who participated in observations and data reduction of SCUSS for their hard work and kind cooperation. The SCUSS is funded by the Main Direc-

tion Program of Knowledge Innovation of Chinese Academy of Sciences (No. KJCX2-EW-T06). It is also an international cooperative project between National Astronomical Observatories, Chinese Academy of Sciences and Steward Observatory, University of Arizona, USA. Technical supports and observational assistances of the Bok telescope are provided by Steward Observatory. The project is managed by the National Astronomical Observatory of China and Shanghai Astronomical Observatory.

Funding for SDSS-III has been provided by the Alfred P. Sloan Foundation, the Participating Institutions, the National Science Foundation, and the U.S. Department of Energy Office of Science. The SDSS-III web site is <http://www.sdss3.org/>.

SDSS-III is managed by the Astrophysical Research Consortium for the Participating Institutions of the SDSS-III Collaboration including the University of Arizona, the Brazilian Participation Group, Brookhaven National Laboratory, Carnegie Mellon University, University of Florida, the French Participation Group, the German Participation Group, Harvard University, the Instituto de Astrofísica de Canarias, the Michigan State/Notre Dame/JINA Participation Group, Johns Hopkins University, Lawrence Berkeley National Laboratory, Max Planck Institute for Astrophysics, Max Planck Institute for Extraterrestrial Physics, New Mexico State University, New York University, Ohio State University, Pennsylvania State University, University of Portsmouth, Princeton University, the Spanish Participation Group, University of Tokyo, University of Utah, Vanderbilt University, University of Virginia, University of Washington, and Yale University.

#### REFERENCES

- An, D., Beers, T. C., Johnson, J. A., et al. 2013, *ApJ*, 763, 65  
 An, D., Beers, T. C., Santucci, R. M., et al. 2015, *ApJ*, 813, L28  
 Abazajian, K., Adelman-McCarthy, J. K., et al. 2004, *AJ*, 128, 502  
 Carollo, D., Beers, T. C., Lee, Y. S., et al. 2007, *Nature*, 450, 1020  
 Carollo, D., Beers, T. C., Chiba, M., et al. 2010, *ApJ*, 712, 692  
 Gu, J. Y., Du, C. H., Jia, Y. P., et al. 2015, *MNRAS*, 452, 3092  
 Gu, J. Y., Du, C. H., et al. 2016, *ApJ*, in press  
 Gunn, J. E., Siegmund, W. A., Mannery, E. J., et al. 2006, *AJ*, 131, 2332  
 Ivezić, Ž., Sesar, B., Jurić, M., et al. 2008, *ApJ*, 684, 287  
 Jurić, M., Ivezić, Ž., Brooks, A., et al. 2008, *ApJ*, 673, 864  
 Jia, Y. P., Du, C. H., Wu, Z. Y., et al. 2014, *MNRAS*, 441, 503  
 Padmanabhan, N., Schlegel, D. J., Finkbeiner, D. P., et al. 2008, *ApJ*, 674, 1217  
 Peng, X. Y., Du, C. H., Wu, Z. Y., 2012, *MNRAS*, 422, 2756  
 Peng, X. Y., Qi, Z. Q., Wu, Z. Y., Ma, J., et al. 2015, *PASP*, 127, 250  
 Schlegel, D. J., Finkbeiner, D. P. & Davis, M. 1998, *ApJ*, 500, 525  
 York, D. G., Adelman, J., Anderson, J. E., Jr., et al. 2000, *AJ*, 120, 1579  
 Zou, H., Zhou, X., Jiang, Z. J., et al., 2015, *AJ*, 150, 104  
 Zou, H., Zhou, X., Jiang, Z. J., et al., 2016, *AJ*, 151, 37  
 Zhao, G., Chen, Y. Q., Shi, J. R., et al. 2006, *Chin. J. Astro. Astrophys.*, 6, 265  
 Zhou, X., Fan, X. H., Fan, Z., et al. 2016, *RAA*, 16, 17